Checking the pH-Induced Conformational Transition of Prion Protein by Molecular Dynamics Simulations: Effect of Protonation of Histidine Residues

Emma Langella,* Roberto Improta,*† and Vincenzo Barone*
*Dipartimento di Chimica, Università Federico II, Complesso Monte S. Angelo, via Cintia, Naples, Italy; and †Istituto di Biostrutture e Bioimmagini-CNR Via Mezzocannone 6, I-80134 Naples, Italy

ABSTRACT The role of acidic pH in the conversion of human prion protein to the pathogenic isoform is investigated by means of molecular dynamics simulations, focusing the attention on the effect of protonation of histidine residues on the conformational behavior of human PrP^C globular domain. Our simulations reveal a significant loss of α-helix content under mildly acidic conditions, due to destructuration of the C-terminal part of HB (thus suggesting a possible involvement of HB into the conformational transition leading to the pathogenic isoform) and a transient lengthening of the native β-sheet. Protonation of His-187 and His-155 seems to be crucial for the onset of the conformational rearrangement. This finding can be related to the existence of a pathogenic mutation, H187R, which is associated with GSS syndrome. Finally, the relevance of our results for the location of a Cu^{2+}-binding pocket in the C-terminal part of the prion is discussed.

INTRODUCTION

According to the ''Protein only hypothesis'' (Griffith, 1967; Prusiner, 1991), the misfolded isoform (PrP^{Sc}) of the normal cellular prion protein (PrP^C) is recognized as the pathogenic agent responsible for the transmissible spongiform encephalopathies, a class of neurodegenerative diseases including scrapie in sheep; bovine spongiform encephalopathy in cattle; and Kuru, CJ Disease, GSS syndrome, and FFI in humans (Prusiner and DeArmond, 1994; Weissmann, 1996). A key event in prion disease pathology appears to be the conformational transition of PrP^C to PrP^{Sc}. PrP^{Sc} is insoluble, partly protease resistant, and its N-terminally truncated form polymerizes into amyloid fibrils (Prusiner et al., 1983; Prusiner, 1991). PrP^C and PrP^{Sc} are chemically indistinguishable (Stahl et al., 1993) but their secondary, tertiary, and quaternary structures differ (Caughey et al., 1991; Stahl and Prusiner, 1991; Pan et al., 1993). PrP^C structure (resolved by means of NMR spectroscopy (Riek et al., 1996, 1997; Donne et al., 1997; Lopez Garcia et al., 2000; Zahn et al., 2000) and more recently by x-ray crystallography (Knaus et al., 2001; Haire et al., 2004)) consists of an unstructured N-terminal region (21–124 aa), a structured core (125–228 aa) including three α-helices (HA, HB, HC spanning residues 144–154, 173–194, and 200–228, respectively for $huPrP^C$), and a short antiparallel β-sheet (formed by two strands, S1 and S2, comprising residues 128–131 and 161–164, respectively, for $huPrP^C$). A stable disulfide bridge connects HB to HC, and there are two glycosylation sites at Asn-181 and Asn-197. The N-terminal region contains an octarepeat (PHGGGWGQ) that has a high affinity for copper ions (Cu^{2+}) (Hornshaw et al., 1995; Stöckel et al., 1998); so it has been hypothesized that PrP^C is involved in copper metabolism (Pauly and Harris, 1998).

PrP^{Sc} is more difficult to characterize because of its insolubility and tendency to aggregate. According to circular dichroism and Fourier transform infrared spectroscopic studies, PrP^{Sc} has a dramatically higher (43% vs. 3%) β-sheet and lower (30% vs. 42%) α-helix content with respect to PrP^C (Pan et al., 1993; Safar et al., 1993). However the precise nature of the key event triggering the conformational transition and the detailed structure of PrP^{Sc} are still unknown. Some experimental studies (Gorodinsky and Harris, 1995; Taraboulos et al., 1995; Harris, 2001) indicate that the conversion to the scrapie isoform may occur on the cell surface. On the other hand, the accumulation of PrP^{Sc} in endosomes of scrapie-infected cells with prevalent acidic pH values (4.0–6.0) (Lee et al., 1996) has suggested that acidic pH could trigger PrP^C conformational transition to PrP^{Sc} (Hornemann and Glockshuber, 1998; Kelly, 1998).

In particular, recent experimental works show that acidic conditions and the presence of a denaturant (urea, guanidine hydrochloride) drive both human PrP(90–231) and murine PrP(121–233) toward a β-sheet rich intermediate, thus highlighting that pH-dependence is an intrinsic property of the C-terminal domain (Swietnicki et al., 1997; Jackson et al., 1999; Hornemann and Glockshuber, 1998). Mildly acidic pH conditions (4.4–6.0) in absence of a denaturant induce a conformational transition of huPrP(90–231) leading to exposure of hydrophobic residues (Swietnicki et al., 1997).

The effect of strongly acidic conditions (glutamic acid, aspartic acid, lysine, arginine, and histidine residues pro-

Submitted March 26, 2004, and accepted for publication July 15, 2004.

Address reprint requests to Vincenzo Barone, Tel.: 39-081-674206; E-mail: baronev@unina.it.

Roberto Improta's permanent address is Istituto di Biostrutture e Bioimmagini-CNR Via Mezzocannone 6, I-80134 Naples, Italy.

Emma Langella's present address is Istituto di Biostrutture e Bioimmagini-CNR Via Mezzocannone 6, I-80134 Naples, Italy.

© 2004 by the Biophysical Society

0006-3495/04/12/3623/10 $2.00

doi: 10.1529/biophysj.104.043448

tonated) on prion conformation has also been recently investigated by molecular dynamics simulations (Alonso et al., 2001, 2002; Sekijima et al., 2003). Daggett and colleagues (Alonso et al., 2001, 2002) studied Syrian hamster, human, and mouse prion proteins, using models including the N-terminal region (107–125 aa), and found that at low pH the protein exhibits a higher conformational mobility and the sheet-like structure increases both by lengthening of the native β-sheet and by addition of a portion of the N-terminus to widen the sheet by two additional strands. Both experimental and computational results thus suggest that a low pH can play a relevant role in modulating the conformational transition to the scrapie isoform.

We further investigate this hypothesis in this study, checking how human PrP^C globular domain reacts to mildly acidic conditions, i.e., much less acidic than that investigated by Alonso et al. (Alonso et al., 2001, 2002) and Sekijima et al. (2003), in which protonation should involve mainly histidine residues. We tackle this goal by means of molecular dynamic (MD) simulations (van Gunsteren and Berendsen, 1990; Braatz et al., 1992; Fox and Kollman, 1996), which have already been fruitfully used to investigate the dynamical behavior of prion proteins (Zuegg and Gready, 1999; Billeter and Wüthrich, 2000; Parchment and Essex, 2000; Alonso et al., 2001, 2002; DeMarco and Daggett, 2004; Santini and Derreumaux, 2004).

In particular, we present the results of several 10 ns MD simulations of the structured core (125–228 aa) of human prion protein in neutral/slightly basic (hereafter PrP_N) and in mildly acidic (hereafter PrP_H) conditions. In PrP_N lysine and arginine are positively charged, glutamic acid and aspartic acid negatively charged, and the four histidines neutral, whereas in PrP_H all the histidines are positively charged, but glutamic acid and aspartic acid remain unprotonated. We decided to focus our attention exclusively on histidine residues because human PrP(90–231) exhibits a conformational change which is complete at pH 4.4 but starts at pH 5.5 (Swietnicki et al., 1997). At that pH it is possible that all the histidine residues are protonated, whereas the same assumption cannot be made for glutamic acid and aspartic acid, whose pK is ~4.3 and ~3.9, respectively, and can be easily decreased by several units (for example, when glutamic acid and aspartic acid are engaged in salt bridges with positively charged residues). It is thus probable that there is a pH range where all histidines are positively charged, whereas most, if not all, of the glutamic acid and aspartic acid residues are still negatively charged. On the other hand, from an experimental point of view, a direct correspondence between histidine protonation state and prion protein conformation is still lacking. As a matter of fact, both NMR and x-ray studies on PrP^C were unable to assess the protonation state of histidine residues. So, our MD simulations could be useful to evaluate the effect of histidine protonation in determining the conformational behavior of human prion protein globular domain. Furthermore, histidines can potentially act as metal coordination sites. Although the presence of copper binding sites beyond the structured core of the protein has been questioned (Burns et al., 2003;), several experimental studies (Cereghetti et al., 2001, 2003; Van Doorslaer et al., 2001) show that the C-ter part of the protein can effectively bind Cu^{2+} ions, and it has been suggested that one of the binding sites contains a histidine residue. However, from an experimental point of view, the precise location of these metal binding sites and the consequence of the metal binding on the prion conformation are still unknown. Binding of a metal cation is obviously a much more complex chemical process than simple protonation (for example it involves more than one residue). Nonetheless, exploring how the protein reacts to the presence of a positive charge in the proximity of a histidine residue could give useful hints on some of the possible effects of metal cation coordination too. Finally, His-187 is involved into a pathogenic mutation associated with GSS syndrome (H187R) (Cervenakova et al., 1999), which implies a positively charged residue in position 187, analogously to His-187 protonation.

Since MD simulations are much more reliable when based on accurate experimental structures, we choose to perform our study on the structured part of the prion, the only one for which unambiguous structural data are available. The exclusion of the 90–124 unstructured N-terminal region avoids errors due to an arbitrary guess for this fragment. This choice, even if preventing us from obtaining relevant conformational changes due to rearrangement of the more flexible N-terminal fragment, should put on a firmer ground all the conclusions drawn from the analysis of our computational results. Furthermore, the structured core of PrP^C, even if not infectious, well represents the characteristic behavior of the full-length prion protein exhibiting an intrinsic pH-dependence and an affinity for metal cations.

METHOD

Both PrP_N and PrP_H MD simulations started from the NMR structure (Zahn et al., 2000) of human PrP(125–228) (PDB entry 1QLX), determined in mildly acidic conditions (pH = 4.5). As mentioned above, in PrP_N lysine and arginine are positively charged, glutamic acid and aspartic acid negatively charged, and all histidines are neutral, whereas in PrP_H all histidines were positively charged, but glutamic acid and aspartic acid remain unprotonated. In both systems the disulphide bond was left intact, as experimental evidences indicate it should be necessary for infectivity (Somerville et al., 1980; Turk et al., 1988; Hermann and Caughey, 1998). Simulations were performed at constant temperature within a fixed-volume box filled with SPC (Berendsen et al., 1981) water molecules by using periodic boundary conditions. The net charges of PrP_N and PrP_H were compensated by adding three Na^+ and one Cl^- ions, respectively. PrP_N simulation includes 20,117 atoms and the PrP_H one 20,843 atoms. The temperature was kept constant at 300 K using the isothermal Gaussian temperature coupling (Brown and Clarke, 1984). LINCS (Hess et al., 1997) was used to constrain bond lengths, allowing a time step of 2 fs. The particle mesh Ewald method (PME) (Darden et al., 1993, 1999) (grid spacing of 0.12 nm) was used for electrostatic calculations, thus properly accounting for long-range interactions. A nonbonded cutoff of 0.9 nm for Lennard-Jones potential was used. For both systems the solvent was relaxed by energy minimization,

followed by 15 ps of MD at 300K, while restraining protein atomic positions with a harmonic potential. The systems were then minimized without restraints and their temperature brought to 300 K in a stepwise manner: 15-ps-long MD runs were carried out at 50, 100, 200, 250, and 300 K before the production runs were started at 300 K. Subsequently both systems were simulated for 10 ns with constrained roto-translational motions (Amadei et al., 2000). Both simulations were performed with the GROMACS simulation package (van der Spoel et al., 1995). A modification of GROMOS87 force field (van Gunsteren and Berendsen, 1987; van Buuren et al., 1993; van Gunsteren et al., 1996), widely and successfully applied to the study of different classes of proteins (de Groot et al., 1998; Grottesi et al., 2002), was used. Although a comparison between different force fields is outside the scope of this study, we point out that recent studies devoted to this aspect indicate that most force fields (including GROMOS96 based on GROMOS87), although providing quite different quantitative results, behave comparably concerning general trends, thus providing a coherent picture of the overall behavior of the system under study (Hu et al., 2003; Mu et al., 2003). Moreover, the force field we have used is widely used by the scientific community and several recent studies convincingly show that it delivers reliable results for a number of biological systems, including peptides and proteins. In the particularly difficult field of folding simulations, the GROMOS96 code (based on the GROMOS87 force field) has provided remarkable results for β-peptides (Daura et al., 1997, 1998, 1999). Secondary structure elements were assigned by the DSSP program (Kabsch and Sander, 1983), whereas INSIGHTII (Accelrys) and MOLMOL (Koradi et al., 1996) programs were used for model manipulation, visual analysis and figure production.

RESULTS

In the following we will use the standard labels HA, HB, HC, and S1, S2 to indicate the three α-helices and the two strands of the β-sheet, respectively. Regions connecting these secondary structure elements (S1, HA, S2, HB, HC) will be referred to as τA, τB, τC, and τD, respectively (see Fig. 1).

Inspection of Fig. 2 reveals that PrP_N is stable during the free dynamic run. The C_α root mean-square deviation (RMSD) increases rapidly within 0.5 ns and then it remains stable at 0.18 nm over the whole simulation period (see Fig. 2). The positions and lengths of the different secondary structure elements of PrP_N are well preserved during the simulation (see Fig. 3) and similar to the initial NMR structure. This result is in agreement with previous

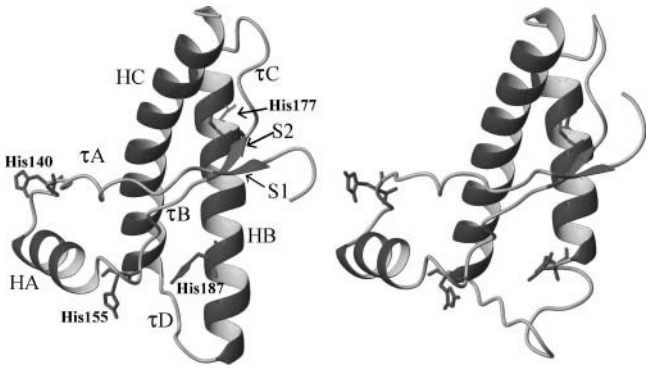

FIGURE 1 Final structures of PrP_N (*left*) and PrP_H (*right*) runs. Labels used to indicate secondary structure elements and connecting regions are also shown. Histidine residues (140, 155, 177, 187) are displayed in sticks.

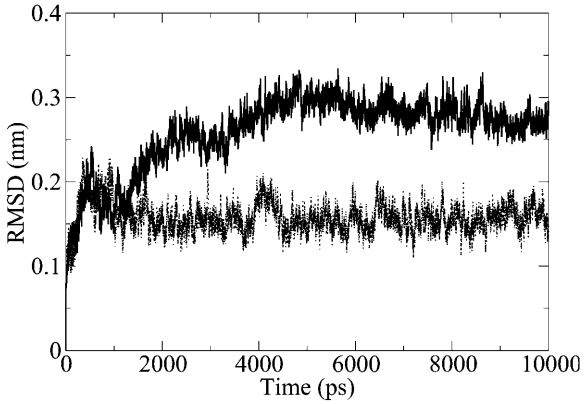

FIGURE 2 Root mean-square deviation of the C_α carbon atoms positions from their positions in the starting NMR structure as a function of time in the PrP_N (*dashed line*) and PrP_H (*solid line*) runs.

MD studies, thus confirming the reliability of the adopted computational protocol. HA, HB, and HC span residues 144–152, 172–194, and 200–226, respectively, whereas S1 and S2 include, on average, residues 129–131 and 161–163, respectively.

On the other hand, protonation of the four histidine residues gives rise to significant conformational changes. As a matter of fact, PrP_H shows a major rearrangement with respect to the starting structure reaching a constant RMSD of 0.28 nm after 6 ns of simulation (see Fig. 2).

An analysis of the secondary structure indicates that HA (residues 144–152) and HC (residues 200–228) are stable throughout the simulation, whereas the C-terminal part (residues 187–194) of HB is highly unstable, undergoing a progressive destructuration during the simulation. In particular, HB loses seven residues, reaching after ~7 ns an equilibrium length spanning residues 172–187, whereas fragment 192–197 exhibits a stable bend structure during the second half of the simulation. Moreover the β-sheet content increases, reaching nine residues during the 4.3–6.1 ns time interval and fluctuating around four to six residues for the remaining simulation time.

The final structures issuing from both simulations are shown in Fig. 1. The key events underlying the conformational behavior of PrP_H are the breaking of the salt bridge between Arg-156 and Glu-196 and the competition between the strongly attractive interactions His-155–Glu-196 and His-187–Glu-196.

During the early stages of the simulation the salt bridge between Arg-156 and Glu-196, present in PrP_N trajectory and recognized as one of the most significant interactions for the stability of the protein by NMR and MD works (Zuegg and Gready, 1999), breaks whereas Glu-196 is engaged into a new salt bridge with His-155. This last salt bridge is stable during the first 6 ns of the simulation (see Fig. 4).

The side chain of His-187 disrupts its hydrogen bond with the carboxylic group of Arg-156, which was stable in PrP_N

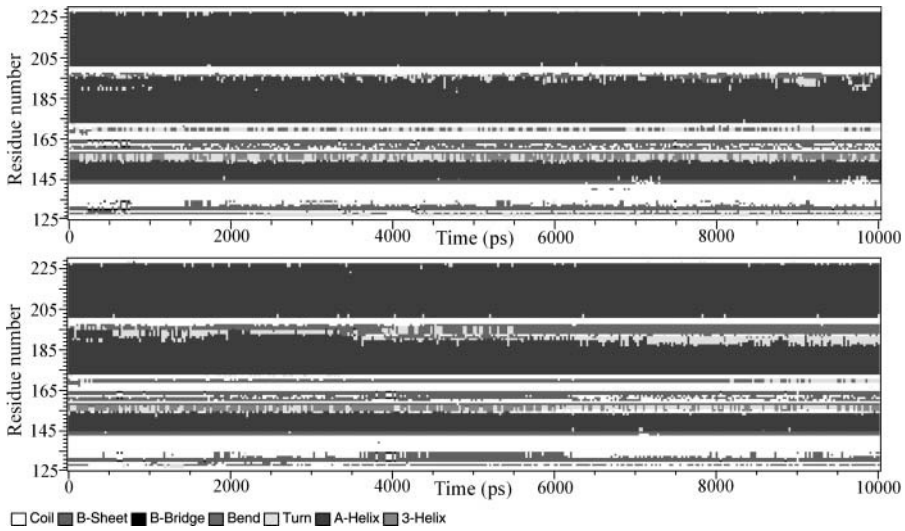

FIGURE 3 Secondary structure of PrP_N (*upper panel*) and PrP_H (*lower panel*) as a function of time, determined with DSSP.

trajectory, and shifts away from the cleft between τB and τD. The His-187 shift is likely responsible for the reorientation of the positively charged N-terminal region (125–127) of the protein (see Fig. 1). This region is indeed directed toward the C-terminus of HB in the NMR structure, as well as in the whole PrP_N simulation. On the contrary, during the first 2 ns of PrP_H simulation it progressively turns to the opposite direction, i.e., toward the N-terminus of HB. This reorientation, that decreases the charge repulsion with His-187, gives rise to a new hydrogen bond between Gly-126 and Pro-165, which is compatible with an elongation of the β-sheet.

The overall PrP_H simulation is governed by the progressive approach of His-187 and Glu-196. However, as mentioned above, during the first half of the simulation the His-155–Glu-196 salt-bridge never breaks (Fig. 4) so that the global process is the approach of three residues (His-187–Glu-196–His-155) which ends up in the formation of a pocket stable between 4.3 and 6.0 ns. It is noteworthy

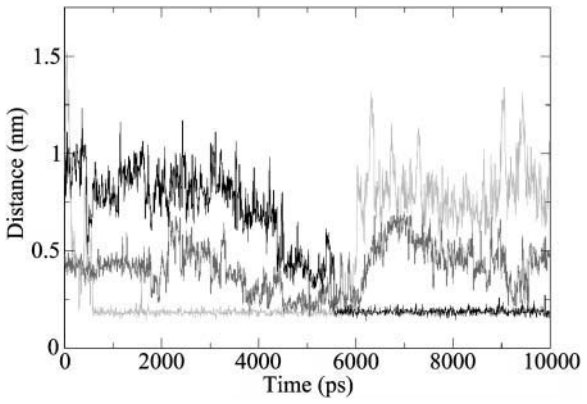

FIGURE 4 Side chains minimum distance between His155 and Glu-196 (*black*) and between His-187 and Glu-196 (*shaded line*) as a function of time in PrP_H trajectory. Distance between Ser-132 carboxylic and Val-161 amidic groups is also shown (*light shaded line*).

that the pocket formation (4.3–6.0 ns) occurs contemporarily to β-sheet elongation (4.2–6.1 ns), through the formation of the hydrogen bond between Ser-132 and Val-161. This latter interaction, that has never been previously reported, appears to play a fundamental role in lengthening and stabilizing the β-sheet between S1 and S2.

Our analysis also reveals the important role played by side chain/main chain interactions in preventing/favoring β-sheet elongation. During β-sheet lengthening, in fact, there is a breaking of the interactions of the side chains of Gln-160 and Asn-159 with the carboxylic group of Gly-131 and Met-134, respectively. On the other hand, between 4.2 and 6.1 ns the carboxylic group of Ser-132 stably binds to Val-161 amidic group, whereas in the remaining time of the simulation (as well as in PrP_N simulation), it strongly interacts with the side chain of Arg-220. The β-sheet lengthening is accompanied by small conformational rearrangements in the whole protein, leading to the formation of new interactions, like e.g., that between Gln-160 and Gln-186.

After 6 ns His-155 breaks its hydrogen bond with Glu-196, whereas Glu-196 remains strongly bound to His-187 for the remaining simulation time. Almost simultaneously, (see Fig. 4) the Ser-132–Val-161 hydrogen bond breaks up, decreasing the β-sheet length. However, it is worth noting that the conformation of several residues (Gly-131, Ser-132, Ala-133) is more extended in PrP_H than in PrP_N for the whole simulation time, making easier transient elongations of the β-sheet made by S1 and S2. In particular, a longer β-sheet is again stable between 9 and 9.5 ns (see Fig. 3). The destructuration process of HB goes on until 7 ns, and in the last 3 ns of the simulation PrP_H does not undergo any significant conformational transition. As we have seen, protonation of His-155 and His-187 seems to play a key role in the conformational transition of PrP_H. Our results suggest instead that this is not the case for His-140 and His-177: in both PrP_N and PrP_H His-140 is stably involved in a salt-bridge with Asp-147, whereas His-177 is always well ex-

posed to the solvent and doesn't seem to affect the overall spatial arrangement of the protein. Furthermore, it is interesting to highlight that, although the NMR experimental structure is more similar to the PrP_N average structure, some local details seem to be better modeled by PrP_H. For example the hydrogen bonds pattern of the region linking τA to HA is characterized by Asp-147–His-140 and Asp-147–Phe-141 hydrogen bonds by both NMR experiments (Zahn et al., 2000) and PrP_H simulation. In PrP_N simulation a third stable hydrogen bond is found between Asp-147 and Gly-142. As a consequence, the local conformation of that region (encompassing His-140) is more similar to the NMR structure in PrP_H than in PrP_N. Those results suggest that His-140 and His-177 might be protonated under NMR experimental conditions.

RESULTS VALIDATION

Since the conformational features exhibited by the PrP_N system during the simulation run are in agreement with both previous experimental (Zahn et al., 2000) and computational (Zuegg and Gready, 1999; Okimoto et al., 2002) studies, we have focused our attention on assessing the statistical significance of the PrP_H simulation and the convergence of the results. To that aim we have performed two other independent 11.4-ns-long test simulations (test1 and test2) differing from PrP_H simulation (hereafter Ref^H) in the starting protein configuration used and in the random seed scheme for velocities attribution employed.

In test1 velocities were redistributed at the beginning of the free-dynamics, whereas in test2 they were redistributed every 700 ps during the free-dynamics. The new starting configuration has been chosen among a set of 20 human prion protein NMR structures (pdb code: 1QLZ) and is the one (model 8) with the highest C_α root mean-square deviation (0.991 Å) with respect to the representative structure (1QLX.pdb) used as starting configuration in Ref^H.

The dynamic picture issuing from test1 and test2 is very similar to that of Ref^H. Both simulations reveal indeed that the system undergoes a significant rearrangement (RMSD $\approx$ 3.0 Å) with respect to the starting configuration, the main event being the progressive HB C-terminal end destructuration (see Fig. 5).

Both simulations are governed by the same interactions previously detected in Ref^H: Glu-198 makes a stable salt-bridge with His-155 thus disrupting the stabilizing interaction with Arg-156; His-187 progressively approaches Glu-196 thus forming a new stable salt-bridge (see Fig. 6).

In test1 those conformational transitions occur with a delay of ~4 ns with respect to Ref^H (and for this reason we slightly increased the simulation time up to 11.4 ns). However, this result is not surprising, due to the different starting model used, and it is meaningful that, apart the aforementioned delay, test1 and Ref^H run almost parallel. The only noticeable difference between test2 and Ref^H is instead a longer persistence of the three center salt-bridge between His-155, His-187, and Glu-198, but this result can also be explained on the basis of the different velocities redistribution scheme used in test2. The agreement between the results of the three simulations performed supports the reliability of our conclusion and puts on a firmer ground all the following considerations.

DISCUSSION AND CONCLUSIONS

In this study we have shown that protonation of the four histidine residues decreases the conformational stability of human PrP(125-228), leading to a significant structural rearrangement (RMSD 3.0 Å) with respect to the starting structure, which involves a decrease in the α-helix and

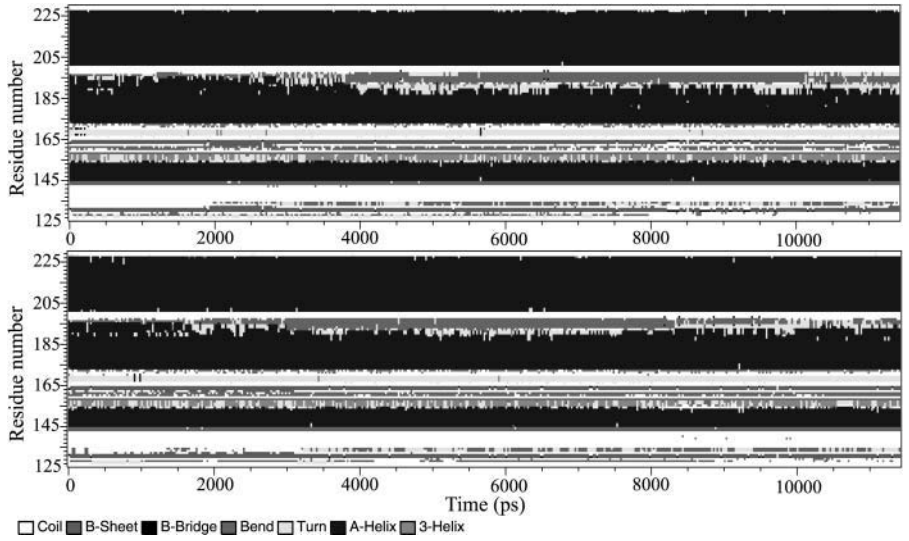

FIGURE 5 Secondary structure of test1 (*upper panel*) and test2 (*lower panel*) as a function of time, determined with DSSP.

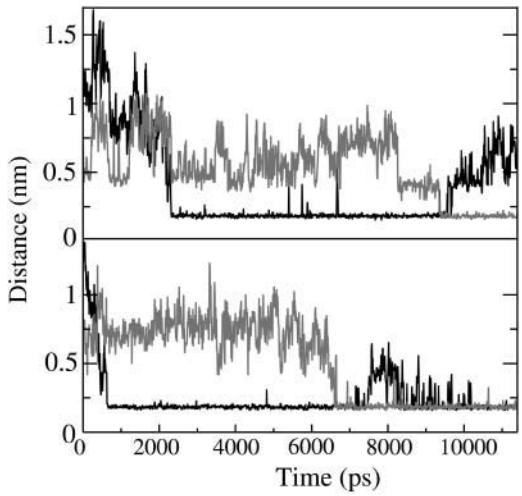

FIGURE 6 Side chains minimum distance between His-155 and Glu-196 (*black line*) and between His-187 and Glu-196 (*gray line*) as a function of time in test1 (*upper panel*) and test2 (*lower panel*) runs.

a transient increase in the β-sheet content. This result is consistent with the experimental finding that murine PrP(121–231) (Hornemann and Glockshuber, 1998) conformation exhibits a significant dependence on pH and human PrP(90–231) undergoes a conformational rearrangement under mildly acidic conditions (pH 4.4–6.0) eventually losing α-helical content upon further pH lowering (Swietnicki et al., 1997).

The most relevant structural changes involve the destructuration of the C-terminal part of helix B (residues 188–194). Until now it has instead been assumed that HB and HC constitute the stable core of the protein whereas the conformational transition to the β-rich form involves helix A (Parchment and Essex, 2000; Alonso et al., 2001). However the results of our computations are in line with NMR (Donne et al. 1997; Zahn et al., 2000) and x-ray (Knaus et al., 2001) data revealing a significant flexibility of the C-terminal end of HB, with a very recent sequence alignment study predicting that the C-terminal residues in HB are frustrated in their helical state (Dima and Thirumalai, 2002), and also with MD simulations by Santini and Derreumaux (2004) which shows that unfolding of HA is not an early step in PrP interconversion and that there is no evidence that HB and HC are more stable than HA. Other recent studies further support the involvement of HB in the conformation transition to the β-rich prion isoform (Gilis and Rooman, 2000; Karlberg et al. 2001; Mornon et al., 2002). This behavior can be relevant also for the development of the infection, since this region belongs to the mini-prion (Muramoto et al., 1996).

Another interesting feature is the transient elongation of the native β-sheet due to the newly formed hydrogen bond between Ser-132 carboxylic and Val-161 amidic groups and likely enhanced by N-terminus reorientation. So, native β-sheet behaves like a nucleation site for a further increase of the β-sheet content, as has been hypothesized in other experimental and computational works (Cohen and Prusiner, 1998; Alonso et al., 2001).

A comparison between our results and those of previous computational studies by Alonso and Daggett is made difficult by the different system they examined (residues 109–228, instead of 125–228) and, especially, by the very different conditions under which the two studies have been performed. Extremely strong acid conditions, involving the protonation of all glutamic acid and aspartic acid residues lead to a breaking of all the salt bridges of the protein and increase its total positive charge up to 17. Such a system is obviously very different from that we have investigated: just to make an example, the Glu-196–His-187 salt bridge (vide infra) would not be possible if Glu-196 is protonated. Anyway we have performed a test MD simulation (15-ns long) of huPrP(125–228) under strongly acidic conditions (glutamic acid, aspartic acid, and histidine protonated) which did not show any significant conformational rearrangement. Indeed, the average C^{α} RMSD during the last 5 ns was 2.5 Å and the secondary structure elements are retained during the whole simulation (see Fig. 1 in supplementary material). These results agree with the MD study performed on huPrP(125–228) by Sekijima et al. (2003), which does not show any dramatic conformational rearrangement under strongly acidic pH conditions. On the other hand these results are not in contrast with Alonso and Daggett ones. As a matter of fact, the work of Alonso and Daggett on huPrP(109–228) shows that the main changes, leading to addition of a portion of the N-terminus to the native β-sheet and to native β-sheet elongation, happen in and are driven by the N-terminal tail (109–124) which is not included in our model as well as in the study by Sekijima et al. (2003).

A detailed analysis of the behavior of the four histidine residues during the simulations reveals that the protonation of His-155 and His-187 is critical for the onset of the conformational transition. In particular the key event leading to the destructuration process of the C-terminal end of HB is the presence of a positive charge on His-187, providing the driving force for the formation of salt bridge with the Glu-196 side chain. This is a crucial point: His-187 is indeed involved in a pathogenic mutation associated with GSS syndrome in human, H187R (Cervenakova et al., 1999), which implies the presence of a positive charge in position 187. Our computational results thus allow us to put forward an explanation for the destabilizing effect of the H187R mutation on the PrP^{C} folding. Intriguingly, there is another well-known pathogenic mutation which places a positive charge in the C-terminus of HB, T188R/K, thus confirming the destabilizing effect of positive charges in that region. On the other hand, His-155 is essential for the breaking of the stabilizing salt bridge between Arg-156 and Glu-196, just in the early stages of the simulation.

A comparison among PrP_N and PrP_H MD simulations and experimental NMR data prompt us to suggest that His-140

and His-177 could be protonated, whereas His-155 and His-187 are neutral under NMR experimental conditions. The more acidic behavior of His-155 and His-187 is qualitatively supported by MEAD computations (pH titrations curves were calculated on the NMR experimental structures by using the MEAD suite (Bashford et al., 1992) and the XMCTI program (Beroza et al., 1991). In MEAD calculations dielectric constants 4.0 and 80.0 for the protein and the solvent, respectively, were used. Atomic radii and partial charges were taken from the PARSE library distributed in MEAD. The individual intrinsic pKa values and the interaction matrix produced by MEAD were input to XCMTI (which uses a Monte Carlo procedure to average over all possible titration microstates of the protein and to calculate the titration curves), predicting that His-140 and His-177 should have $pK_a \geq 7$, whereas His-155 and His-187 should be protonated only for pH <5. At this pH values it could be obviously possible that other protonable residues as aspartic acid and glutamic acid undergo protonation; however our MEAD calculations suggest that the only residues having pKs close to five are located at the C-ter of Helix C, i.e., in a region not involved in the most significant conformational transition of PrP_H. Furthermore, according to our simulations the only acid residue whose protonation is expected to influence our results is Glu-196. However, our study, in agreement with previous experimental and computational studies (Zuegg and Gready, 1999), shows that before His-187 protonation this residue should be salt-bridged with Arg-156, and thus its pK_a is expected to be significantly <4.5.

Our simulations could also be useful to corroborate the results of a very recent electron paramagnetic resonance (EPR) study of ad hoc designed murine prion mutants strongly suggesting that His-187 is involved in one of the copper binding sites of PrP^C (Cereghetti et al., 2001, 2003; Van Doorslaer et al., 2001). However it was not possible to determine the whole coordination site. Nonetheless, copper binding is not predicted to give rise to substantial conformational changes. PrP^H simulation shows that a conformational transition does exist, leading three possible Cu^{2+} ligands (Glu-196, His-155, and His-187) to point toward the same region, the cleft between τB and τD, that is well solvent exposed (see Fig. 7).

Small changes in the side chain conformations could then easily allow to accommodate a copper ion. Can the presence of a Cu^{2+} ion, under physiological conditions, be the driving force for a conformational change like the one caused by histidine protonation? Only calculations performed in the presence of Cu^{2+} ion could obviously give a definite answer to the above question. However our results suggest what conformational transition allows His-187 to be approached by additional ligands without dramatic changes in the overall conformation of the prion, apart from some partial unfolding of the C-ter part of Helix B.

According to our simulation, His-187 and Glu-196 are thus the most probable candidates for being the binding

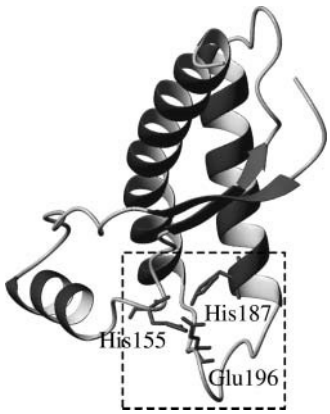

FIGURE 7 PrP_H structure at 5.5 ns. Lengthening of native β-sheet can be observed. Residues His-155, His-187, and Glu-196 are displayed in stick.

residues of Cu^{2+}, but it cannot be excluded that in human PrP^C also His-155 is involved. Since murine prion protein has only three histidine residues (His-140, His-177, and His-187), the EPR data of Cereghetti et al. (2001, 2003) cannot shed light on this question. Interestingly, NMR experiments on human PrP^C suggest that region 153–159, centered on His-155, is influenced by the metal binding (Jackson, et al. 2001). A comparative EPR analysis of copper binding to the C-terminal domain of human PrP^C would therefore be very interesting: eventually, the discovery of different, species-dependent, specific metal-prion complexes could have significant implications for a better understanding of prion deseases species barrier.

The possible involvement of His-187 in the metal binding allows to propose an alternative explanation to the pathogenic mutation H187R, that (besides having a role in HB C-terminal part destructuration) could play some role in preventing copper binding too. The existence of another pathogenic mutation close to the region we propose as a copper binding site, F198S, which has been experimentally proven (Cereghetti et al., 2001, 2003; Van Doorslaer et al., 2001) to keep copper from binding to His-187, further supports the hypothesis that PrP^C pathogenic mutations could be related to altered Cu(II) binding.

Due to the complexity of the phenomena under study, it is not easy to assess the relevance of our results for characterizing the structure of the experimentally detected unfolding intermediate of PrP^C (Apetri and Surewicz, 2002), and, more in general, the conformational transition from PrP^C to PrP^{Sc}. On one hand, we have studied the structured part of an isolated human prion protein. Several intramolecular and intermolecular interactions cannot be taken into account by our simulations, and they could be fundamental for the stabilization of the PrP^{Sc}. Furthermore, our model lacks N-linked glycosylation sites which could play a role in the conformational transition mechanism. Finally, many different effects and kinds of interactions have been predicted to modulate the conformational behavior of

the prion protein: it is thus sure that the protonation of four histidine residues, and even the decrease of the pH alone, cannot be considered the only important effects able to destabilize α-helical and to stabilize β-sheet structures in prions.

On the other hand, experiments show that the prion conformational rearrangement due to pH decrease starts already under mildly acid conditions, suggesting that histidine can play a relevant role in this phenomenon. Our study points out that this is the case: the simple protonation of the histidine residues might trigger a conformational transition involving a significant decrease of α-helical content and the stabilization of extended structures. The analysis of the MD results, showing that the protonation of two histidine residues (His-187 and His-155) could be the main cause of this transition, not only provides insights on some key microscopic events giving account of the pH influence on prion conformation, but suggests which are the ''intrinsic'' instability lines of the protein. The region comprising the C-ter part of HA and HB, τB and τD is predicted to be extremely sensitive to the presence of extra-positive charges, and conformational rearrangements in that region (e.g., the formation of the transient pocket depicted in Fig. 7) can propagate through the protein leading to the β-sheet lengthening. From this point of view, it could be significant that some important pathogenic mutations (H187R, T188R/K, E200K, D202N) involve the appearance of positively charged and/or the disappearance of negatively charged residues in that region or in its proximity. The effect of those mutations could obviously be significant for interprotein interactions. However, our results suggest that, even if such mutations do not alter significantly the thermodynamic stability of the folded state, they could increase the stability of unfolding intermediates with a decreased α-helical content and longer and more stable β-sheet, which constitute the main structural differences between PrP^{C} and PrP^{Sc}.

SUPPLEMENTARY MATERIAL

An online supplement to this article can be found by visiting BJ Online at http://www.biophysj.org.

We are grateful to Dr. Orlando Crescenzi for performing MEAD computations. We thank Prof. Alfredo Di Nola and Dr. Riccardo Spezia for advice on the simulations and for useful discussions.

This work was supported by the Italian Ministry for the University and the Scientific and Technological Research (grant 2001031717-005).

REFERENCES

Alonso, D. O. V., C. An, and V. Daggett. 2002. Simulations of biomolecules: characterization of the early steps in the pH-induced conformational conversion of the hamster, bovine and human forms of the prion protein. *Philos. Trans. R. Soc. Lond. A.* 360:1165–1178.

Alonso, D. O. V., S. J. DeArmond, F. E. Cohen, and V. Daggett. 2001. Mapping the early steps in the pH-induced conformational conversion of the prion protein. *Proc. Natl. Acad. Sci. USA.* 98:2985–2989.

Amadei, A., G. Chillemi, M. A. Ceruso, A. Grottesi, and A. Di Nola. 2000. Molecular dynamics simulations with constrained roto-translational motions: Theoretical basis and statistical mechanical consistency. *J. Chem. Phys.* 112:9–23.

Apetri, A. C., and W. K. Surewicz. 2002. Kinetic intermediate in the folding of human prion protein. *J. Biol. Chem.* 277:44589–44592.

Bashford, D. and K. Gerwert. 1992. Electrostatic calculations of the pKa values of ionizable groups in bacteriorhodopsin. *J. Mol. Biol.* 224:473–486.

Berendsen, H. J. C., J. P. M. Postma, W. F. van Gunsteren, and J. Hermans. 1981. Interaction models for water in relation to protein hydration. *In* Intermolecular Forces. Reidel, Dordrecht, Germany. 331–342.

Beroza, P., D. R. Fredkin, M. Y. Okamura, and G. Fehler. 1991. Protonation of interacting residues in a protein by a Monte Carlo method: application to lysozyme and the photosynthetic reaction center of Rhodobacter sphaeroides. *Proc. Natl. Acad. Sci. USA.* 88:5804–5808.

Billeter, M., and K. Wüthrich. 2000. The prion protein globular domain and disease-related mutants studied by molecular dynamics simulations. *Arch. Virol.* 16:251–263.

Braatz, J. A., M. D. Paulsen, and R. L. Ornstein. 1992. 3 Nsec molecular dynamics simulation of the protein ubiquitin and comparison with x-ray crystal and solution NMR structures. *J. Biomol. Struct. Dyn.* 9:935–949.

Brown, D., and J. H. R. Clarke. 1984. A comparison of constant energy, constant temperature, and constant pressure ensembles in molecular dynamics simulations of atomic liquids. *Mol. Phys.* 51:1243–1252.

Burns, C. S., E. Aronoff-Spencer, G. Legname, S. B. Prusiner, W. E. Antholine, G. J. Gerfen, J. Peisach, and G. L. Millhauser. 2003. Copper coordination in the full-length, recombinant prion protein. *Biochemistry.* 42:6794–6803.

Caughey, B. W., A. Dong, K. S. Bhat, D. Ernst, S. F. Hayes, and W. S. Caughey. 1991. Secondary structure analysis of the scrapie-associated protein PrP 27–30 in water by infrared spectroscopy. *Biochemistry.* 30: 7672–7680.

Cereghetti, M. G., A. Schweiger, R. Glockshuber, and S. Van Doorslaer. 2001. Electron paramagnetic resonance evidence for binding of Cu2+ to the C-terminal domain of the murine prion protein. *Biophys. J.* 81:516–525.

Cereghetti, G. M., A. Schweiger, R. Glockshuber, and S. Van Doorslaer. 2003. Stability and Cu(II) binding of prion protein variants related to inherited human prion diseases. *Biophys. J.* 84:1985–1997.

Cervenakova, L., C. Buetefisch, I. Taller, H.-S. Lee, G. Stone, C. J. J. Gibbs, P. Brown, M. Hallett, and L. G. Goldfarb. 1999. Novel PRNP sequence variant associated with familial encephalopathy. *Am. J. Med. Genet.* 88:653–656.

Cohen, F. E., and S. B. Prusiner. 1998. Pathologic conformations of prion proteins. *Annu. Rev. Biochem.* 67:793–819.

Darden, T., L. Perera, L. Li, and L. Pedersen. 1999. New tricks for modelers from the crystallography toolkit: the particle mesh Ewald algorithm and its use in nucleic acid simulations. *Structure.* 7:R55–R60.

Darden, T., D. York, and L. Pedersen. 1993. Particle mesh Ewald: an N×log(N) method for Ewald sums in large systems. *J. Chem. Phys.* 98:10089–10092.

Daura, X., B. Jaun, D. Seebach, W. F. van Gunsteren, and A. E. Mark. 1998. Reversible peptide folding in solution by molecular dynamics simulation. *J. Mol. Biol.* 280:925–932.

Daura, X., W. F. van Gunsteren, and A. E. Mark. 1999. Folding-unfolding thermodynamics of a b-heptapeptide from equilibrium simulations. *Proteins.* 34:269–280.

Daura, X., W. F. van Gunsteren, D. Rigo, B. Jaun, and D. Seebach. 1997. Studying the stability of a helical b-heptapeptide by molecular dynamics simulations. *Chem. Eur. J.* 3:1410–1417.

de Groot, B. L., S. Hayward, D. M. F. van Aalten, A. Amadei, and H. J. C. Berendsen. 1998. Domain motions in bacteriophage T4 lysozyme: a comparison between molecular dynamics and crystallographic data. *Proteins.* 31:116–127.

DeMarco, M. L., and V. Daggett. 2004. From conversion to aggregation: protofibril formation of the prion protein. *Proc. Natl. Acad. Sci. USA.* 101:2293–2298.

Dima, R. I., and D. Thirumalai. 2002. Exploring the propensities of helices in PrP(C) to form beta sheet using NMR structures and sequence alignments. *Biophys. J.* 83:1268–1280.

Donne, D. G., J. H. Viles, D. Groth, I. Mehlhorn, T. L. James, F. E. Cohen, S. B. Prusiner, P. E. Wright, and H. J. Dyson. 1997. Structure of the recombinant full-length hamster prion protein PrP(29–231): the N terminus is highly flexible. *Proc. Natl. Acad. Sci. USA.* 94:13452–13457.

Fox, T., and P. A. Kollman. 1996. The application of different solvation and electrostatic models in molecular dynamics simulations of ubiquitin: how well is the x-ray structure ''maintained''? *Proteins.* 25:315–334.

Gilis, D., and M. Rooman. 2000. PoPMuSic, an algorithm for predicting protein mutant stability changes. Application to prion protein. *Protein Eng.* 13:849–856.

Gorodinsky, A., and D. A. Harris. 1995. Glycolipid-anchored proteins in neuroblastoma cells form detergent-resistant complexes without caveolin. *J. Cell Biol.* 129:619–627.

Griffith, J. S. 1967. Self-replication and scrapie. *Nature.* 215:1043–1044.

Grottesi, A., M.-A. Ceruso, A. Colosimo, and A. Di Nola. 2002. Molecular dynamics study of a hyperthermophilic and a mesophilic rubredoxin. *Proteins.* 46:287–294.

Haire, L. F., S. M. Whyte, N. Vasisht, A. C. Gill, C. Verma, E. J. Dodson, G. G. Dodson, and P. M. Bayley. 2004. The crystal structure of the globular domain of sheep prion protein. *J. Mol. Biol.* 336:1175–1183.

Harris, D. A. 2001. Biosynthesis and cellular processing of the prion protein. *Adv. Protein Chem.* 57:203–228.

Hermann, L. M., and B. Caughey. 1998. The importance of the disulfide bond in prion protein conversion. *Neuroreport.* 9:2457–2461.

Hess, B., H. Bekker, H. J. C. Berendsen, and J. G. E. M. Fraaije. 1997. LINCS: a linear constraint solver for molecular simulations. *J. Comput. Chem.* 18:1463–1472.

Hornemann, S., and R. Glockshuber. 1998. A scrapie-like unfolding intermediate of the prion protein domain PrP(121–231) induced by acidic pH. *Proc. Natl. Acad. Sci. USA.* 95:6010–6014.

Hornshaw, M. P., J. R. McDermott, and J. M. Candy. 1995. Copper binding to the N-terminal tandem repeat regions of mammalian and avian prion protein. *Biochem. Biophys. Res. Commun.* 207:621–629.

Hu, H., M. Elstner, and J. Hermans. 2003. Comparison of a QM/MM force field and molecular mechanics force fields in simulations of alanine and glycine ''dipeptides'' (Ace-Ala-Nme and Ace-Gly-Nme) in water in relation to the problem of modeling the unfolded peptide backbone in solution. *Proteins.* 50:451–463.

Jackson, G. S., A. F. Hill, C. Joseph, L. Hosszu, A. Power, J. P. Waltho, A. R. Clarke, and J. Collinge. 1999. Multiple folding pathways for heterologously expressed human prion protein. *Biochim. Biophys. Acta.* 1431:1–13.

Jackson, G. S., I. Murray, L. L. P. Hosszu, N. Gibbs, J. P. Waltho, A. R. Clarke, and J. Collinge. 2001. Location and properties of metal-binding sites on the human prion protein. *Proc. Natl. Acad. Sci. USA.* 98:8531–8535.

Kabsch, W., and C. Sander. 1983. Dictionary of protein secondary structure: pattern recognition of hydrogen-bonded and geometrical features. *Biopolymers.* 2577–2637.

Karlberg, Y., M. Gustafsson, B. Persson, J. Thyberg, and J. Johanson. 2001. Prediction of amyloid fibril-forming proteins. *J. Biol. Chem.* 276:12945–12950.

Kelly, J. W. 1998. The environmental dependency of protein folding best explains prion and amyloid diseases. *Proc. Natl. Acad. Sci. USA.* 95: 930–932.

Knaus, K. J., M. Morillas, W. Swietnicki, M. Malone, W. Surewicz, and V. C. Yee. 2001. Crystal structure of the human prion protein reveals a mechanism for oligomerization. *Nat. Struct. Biol.* 8:770–774.

Koradi, R., M. Billeter, and K. Wüthrich. 1996. MOLMOL: a program for display and analysis of macromolecular structures. *J. Mol. Graph.* 14: 51–55.

Lee, R. J., S. Wang, and P. S. Low. 1996. Measurement of endosome pH following folate receptor-mediated endocytosis. *Biochim. Biophys. Acta.* 1312:237–242.

Lopez Garcia, F., R. Zhan, R. Riek, and K. Wüthrich. 2000. NMR structure of the bovine prion protein. *Proc. Natl. Acad. Sci. USA.* 97:8334–8339.

Mornon, J.-P., K. Prat, F. Dupuis, N. Boisset, and I. Collebaut. 2002. Structural features of prions explored by sequence analysis. II. A PrPSc model. *Cell. Mol. Life Sci.* 59:2144–2154.

Mu, Y., D. S. Kosov, and G. Stock. 2003. Conformational dynamics of trialanine in water. 2. Comparison of AMBER, CHARMM, GROMOS, and OPLS force fields to NMR and infrared experiments. *J. Phys. Chem. B.* 107:5064–5073.

Muramoto, T., M. Scott, F. E. Cohen, and S. B. Prusiner. 1996. Recombinant scrapie-like prion protein of 106 amino acids is soluble. *Proc. Natl. Acad. Sci. USA.* 93:15457–15462.

Okimoto, N., K. Yamanaka, A. Suenaga, M. Hata, and T. Hoshino. 2002. Computational studies on prion proteins: effect of Ala(117)Val mutation. *Biophys. J.* 82:2746–2757.

Pan, K. M., M. Baldwin, J. Nguyen, M. Gasset, A. Serban, D. Groth, Z. Huang, R. J. Fletterick, F. E. Cohen, and S. B. Prusiner. 1993. Conversion of α-helixes into β-sheets features in the formation of the scrapie prion proteins. *Proc. Natl. Acad. Sci. USA.* 90:10962–10966.

Parchment, O. G., and J. W. Essex. 2000. Molecular dynamics of mouse and Syrian hamster PrP: implications for activity. *Proteins.* 38:327–340.

Pauly, P. C., and D. A. Harris. 1998. Copper stimulates endocytosis of the prion protein. *J. Biol. Chem.* 273:33107–33110.

Prusiner, S. B. 1991. Molecular biology of prion diseases. *Science.* 252: 1515–1522.

Prusiner, S. B., and S. J. DeArmond. 1994. Prion diseases and neurodegeneration. *Annu. Rev. Neurosci.* 17:311–339.

Prusiner, S. B., M. P. McKinley, K. A. Bowman, D. C. Bolton, P. E. Bendheim, D. F. Groth, and G. G. Glenner. 1983. Scrapie prions aggregate to form amyloid-like birefringent rods. *Cell.* 35:349–358.

Riek, R., S. Hornemann, G. Wider, M. Billeter, R. Glockshuber, and K. Wüthrich. 1996. NMR structure of the mouse prion protein domain PrP(121–231). *Nature.* 382:180–182.

Riek, R., S. Hornemann, G. Wider, R. Glockshuber, and K. Wüthrich. 1997. NMR characterization of the full-length recombinant murine prion protein, mPrP(23–231). *FEBS Lett.* 413:282–288.

Safar, J., P. P. Roller, D. C. Gajdusek, and C. J. Gibbs, Jr. 1993. Thermal stability and conformational transitions of scrapie amyloid (prion) protein correlate with infectivity. *Protein Sci.* 2:2206–2216.

Santini, S., and P. Derreumaux. 2004. Helix H1 of the prion protein is rather stable against environmental perturbations: molecular dynamics of mutation and deletion variants of PrP(90–231). *Cellular and molecular life sciences. Cell. Mol. Life Sci.* 61:951–960.

Sekijima, M., C. Motono, S. Yamasaki, K. Kaneko, and Y. Akiyama. 2003. Molecular dynamics simulation of dimeric and monomeric forms of human prion protein: insight into dynamics and properties. *Biophys. J.* 85:1176–1185.

Somerville, R. A., G. C. Millson, and R. H. Kimberlin. 1980. Sensitivity of scrapie infectivity to detergents and 2-mercaptoethanol. *Intervirology.* 13:126–129.

Stahl, N., M. A. Baldwin, D. B. Teplow, L. Hood, B. W. Gibson, A. L. Burlingame, and S. B. Prusiner. 1993. Structural studies of the scrapie prion protein using mass spectrometry and amino acid sequencing. *Biochemistry.* 32:1991–2002.

Stahl, N., and S. B. Prusiner. 1991. Prions and prion proteins. *FASEB J.* 5:2799–2807.

Stöckel, J., J. Safar, A. C. Wallace, F. E. Cohen, and S. B. Prusiner. 1998. Prion protein selectively binds copper(II) ions. *Biochemistry.* 37:7185–7193.

Swietnicki, W., R. Petersen, P. Gambetti, and W. K. Surewicz. 1997. pH-dependent stability and conformation of the recombinant human prion protein PrP(90–231). *J. Biol. Chem.* 272:27517–27520.

Taraboulos, A., M. Scott, A. Semenow, D. Avraham, L. Laszlo, and S. B. Prusiner. 1995. Cholesterol depletion and modification of COOH-terminal targeting sequence of the prion protein inhibit formation of the scrapie isoform. *J. Cell Biol.* 129:121–132.

Turk, E., D. B. Teplow, L. E. Hood, and S. B. Prusiner. 1988. Purification and properties of the cellular and scrapie hamster prion proteins. *Eur. J. Biochem.* 176:21–30.

van Buuren, A. R., S. J. Marrink, and H. J. C. Berendsen. 1993. A molecular dynamics study of the decane/water interface. *J. Phys. Chem.* 97:9206–9212.

van der Spoel, D., A. R. van Buuren, E. Apol, P. J. Meulenhoff, D. P. Tieleman, A. L. Sijbers, B. Hess, K. A. Feenstra, E. Lindahl, R. van Drunen, and H. J. C. Berendsen. 2001. GROMACS User Manual, Version 3.0. Nijenborgh, AG Groningen, The Netherlands. Internet: www.gromacs.org.

Van Doorslaer, S., G. M. Cereghetti, R. Glockshuber, and A. Schweiger. 2001. Unraveling the Cu^{2+} Binding sites in the C-terminal domain of the murine prion protein: a pulse EPR and ENDOR study. *J. Phys. Chem. B.* 105:1631–1639.

van Gunsteren, W. F., and H. J. C. Berendsen. 1987. Groningen Molecular Simulation (GROMOS) Library Manual. Biomos, Groningen, The Netherlands.

van Gunsteren, W. F., and H. J. C. Berendsen. 1990. Computer simulation of molecular dynamics: methodology, applications and perspectives in chemistry. *Angew. Chem. Int. Ed. Engl.* 29:992–1023.

van Gunsteren, W. F., S. Billeter, A. Eising, P. H. Hunenberger, P. Kruger, A. E. Mark, W. R. P. Scott, and I. G. Tironi. 1996. Biomolecular Simulation: The GROMOS96 Manual and User Guide. BIOMOS b.v., Groninger, Zurich, Switzerland.

Weissmann, C. 1996. The ninth datta lecture. Molecular biology of transmissible spongiform encephalopathies. *FEBS Lett.* 21:482–487.

Zahn, R., A. Liu, T. Luhrs, R. Riek, C. von Schroetter, F. Garcia, M. Billeter, L. Calzolai, G. Wider, and K. Wüthrich. 2000. NMR solution structure of the human prion protein. *Proc. Natl. Acad. Sci. USA.* 97:145–150.

Zuegg, J., and J. E. Gready. 1999. Molecular dynamics simulations of human prion protein: importance of correct treatment of electrostatic interactions. *Biochemistry.* 38:13862–13876.